09,08

Mutual transformation of the light waves by contra-directional mixing on reflection holographic grating in $Bi_{12}SiO_{20}$ crystal of (001)-cut

© V.N. Naunyka, A.V. Makarevich

Shamyakin Mozyr State Pedagogical University,
Mozyr, Belarus

E-mail: valnav@inbox.ru

Received November 2, 2022
Revised December 23, 2022
Accepted December 23, 2022

The features of energy exchange during the contra-directional mixing of two linearly polarized light waves in a cubic photorefractive $Bi_{12}SiO_{20}$ piezocrystal of (001)-cut are analyzed. The dependences of the relative intensity of the signal wave on the azimuth of its polarization at the entrance to the crystal during mixing with the reference wave polarized in the plane of incidence are theoretically studied for various crystal orientation angles. The dependence of the relative intensity of the signal wave on the azimuth of its polarization is experimentally studied for the cases when the vector amplitudes of light waves propagating in the crystal are parallel and perpendicular to each other. The calculation is based on the numerical solution of the coupled waves equations with and without taking into account the self-diffraction of the light waves by the reflection holographic grating recorded in the crystal. Based on a comparison of theoretical and experimental data, the influence of self-diffraction on the mutual transformation of light waves during their contra-directional mixing is analyzed. The limits of applicability of the static grating and the dynamic grating approximations for solution of the coupled waves equations are determined.

Keywords: Photorefractive crystal, reflection holographic grating, coupled wave equations, self-diffraction.

DOI: 10.21883/PSS.2023.03.55587.516

1. Introduction

The problem of mutual transformation of two light waves with their contra-directional interaction in cubic photorefractive crystals has been considered in sufficient details by a number of authors (see, for example, the analytical review in [1]). Due to relatively short time of the photorefractive response and high light-sensitivity, these crystals are used as photosensitive media in optic signal transmitting and processing devices, adaptive holographic interferometers, controlled optical filters, integrated optical modulators, etc. [2,3].

When modelling the interaction of light waves in cubic photorefractive crystals, it should be taken into account that in addition to the linear electrooptic effect the dielectric permittivity of crystal at optical frequencies can be additionally modulated due to the combined contribution from photoelastic and inverse piezoelectric effects. This is because of the role of elastic deformations that accompany the electric fields induced in the photorefractive piezocrystal [4]. Analytic expressions to calculate changes in components of the inverse tensor of dielectric permittivity of a cubic crystal taking into account linear electrooptic, photoelastic and inverse piezoelectric effects are presented in [5]. The expressions derived in the study can be used to calculate coupling coefficients in coupled-wave equations and to find out the dependence of energy and polarization characteristics of diffracted light on the orientation of hologram wave vector in the crystallographic coordinate system.

The anisotropy of the photorefractive effect in cubic crystals of 23 and $\bar{4}3m$ symmetry classes with consideration to the photoelastic effect is studied theoretically and experimentally in [6]. Orientations are found for the holographic grating wave vector lying in the plane (110) relative to the crystallographic direction $[1\bar{1}0]$, which yield the highest efficiency of self-diffraction of the light waves on dynamic holograms. Coupled-wave equations suitable for modelling the diffraction of a light wave on a phase holographic grating in a cubic photorefractive crystal of the 23 symmetry class and obtained with consideration to the linear electrooptic, photoelastic, inverse piezoelectric effects, as well as the optical activity are presented in [7]. This study investigates the dependence of diffraction efficiency of a hologram on the orientation angle of a $(\bar{1}10)$ cut crustal and the input polarization azimuth of the light wave. It is shown that the consideration of inverse piezoelectric effect and optical activity lies behind the coincidence between experimental data and results of the theoretical calculations obtained on the basis of analytic solution to the coupled-wave equations. Investigations aimed at studying properties of the holographic gratings formed in cubic optically active photorefractive piezocrystals are reviewed in [8].

The presence of vacancies for silicon, titanium and germanium, respectively, in undoped cubic photorefractive crystals of sillenite type, $Bi_{12}SiO_{20}$ (BSO), $Bi_{12}TiO_{20}$ (BTO), $Bi_{12}GeO_{20}$ (BGO), together with photoconductivity is responsible for the manifestation of a noticeable circular dichroism in them [9]. The technique to determine the parameter of circular dichroism in an optically active

absorbing isotropic medium or a cubic crystal is proposed in [10]. The circular dichroism can have a significant effect on the diffraction efficiency of transmission holograms formed in cubic photorefractive piezocrystals [11]. Results of studying features of the effect of natural absorption and circular dichroism in the drift mode on the gain in case of two-wave mixing in the transmission geometry for the BSO crystal are presented in [12]. It is shown theoretically that taking into account the circular dichroism results in a change in the orientation angles that yield the highest gain of a transmission hologram. Laws of the circular dichroism effect on the diffraction efficiency of the reflection hologram formed in the BSO crystal are studied in [13]. This study theoretically determines the parameters of crystal (thickness, cut) and polarization of the reading light wave at which the diffraction efficiency of reflection hologram in the BSO crystal can achieve the highest value.

The effect of self-diffraction of light waves and parameters of the holographic grating formed in the photorefractive crystal can be investigated using various techniques [14–17]. An accurate solution to the nonlinear equations intended to calculate self-diffraction of two light waves on a local photorefractive grating formed in a photorefractive crystal of the $\bar{4}3m$ symmetry class is obtained in [14]. It is shown that the efficiency of energy exchange between coupled waves and the state of their polarization have a periodic dependence on the reduced length of interaction. A technique to calculate the gain with a two-wave mixing in the optically active photorefractive BSO crystal in the diffusion mode taking into account the effect of self-diffraction of light waves is presented in [15]. The proposed technique is based on integrating the signal wave amplitude over the thickness of the crystal specimen and generates interest in it due to the possibility to take into account the effect of optical activity on coupling coefficients between the light waves mixing on the dynamic grating. In [16], the matrix method was applied to calculate the spectrum of signal beam intensity oscillations at anisotropic self-diffraction of phase-modulated beams in a gyrotropic photorefractive crystal. It is shown that spectrum of such oscillations at local and nonlocal responses of the crystal depends to a significant extent on the polarization of recording wave. In [17], the method of digital holography was used to measure the period and reconstruct the holographic grating formed at self-diffraction of light waves in an anisotropic photorefractive crystal.

Features of the self-diffraction of light waves in photorefractive crystals had been considered by a number of authors in recent publications [18–20]. Results of experimental observation of the frequency-modulated light self-diffraction in the photorefractive BTO crystal are presented in [18]. It is shown that as a result of light self-diffraction on a uniformly accelerated moving hologram a change in the power of light beams at the output of the crystal takes place in the form of chirp-pulse, which can be used to determine photoelectric parameters of high band gap semiconductors. The possibility to control the direction of energy transfer at self-diffraction of higher-order light beams in photorefractive crystals with a sillenite structure is studied in [19]. The authors have analyzed the laws of energy exchange between light beams at a change in the phase shift between the fringe pattern and the holographic grating for the case of two-wave mixing in the transmission geometry. Features of the self-diffraction of 2D light beams with different distributions of intensities are analyzed in a recent study [20]. The differences are studied in the propagation of Gaussian and super-Gaussian 2D light beams, advantages and disadvantages are noted for the use of square and cylindrical light beams with super-Gaussian distribution of intensity. The possibility to achieve the quasi-soliton mode of light beams propagation at relatively low levels of external electric field strengths is found.

When considering the contra-directional mixing of linearly polarized light waves in a cubic photorefractive crystal, the majority of studies (see, for example, [21–23]) analyze the case when vector amplitudes of the reference and object waves are parallel to each other during the propagation inside the crystal. In [21], an analytical expression is obtained to calculate the gain of reflection hologram and it is shown that this gain achieves the highest level in the case when vector amplitudes of light waves coincide and are at a small angular distance from the semi-axis of the ellipse of the optical indicatrix central cross-section, which corresponds to a refractive index of $n_0 + \Delta n$, where n_0 being refractive index of an unperturbed crystal, Δn being the change in the refractive index corresponding to the amplitude of the holographic grating. A more general case is considered in [22], where analytical expressions are presented to calculate the gain of reflection hologram and its diffraction efficiency. Also, this study discusses the conditions of holographic experiment that yield the highest levels of output energy characteristics of reflection hologram in the (001) cut BSO crystal. A similar problem with consideration to the photoelastic and inverse piezoelectric effects, as well as the optical activity, is solved in [23]. Expressions are obtained to calculate components of the vector amplitude of light waves in the case of photorefractive crystal of the 23 symmetry and arbitrary cut and curves of dependencies of reflection hologram energy characteristics on the thickness of specimens of (001) and (111) cuts are analyzed.

Despite a fairly large number of publications devoted to the topic of this study, the following question remains open: what conditions of the holographic experiment are needed to realize the optimum mode of self-diffraction of light waves on the holographic grating formed in a photorefractive crystal, for which the highest intensity of the object wave is achieved in the case of contra-directional two-wave mixing. It is interesting to analyze the general case when vector amplitudes of light waves, during their propagation in the crystal, are oriented arbitrarily to each other. Such an investigation would allow us to evaluate the effect of choice of the polarization azimuth of light waves on the direction of energy exchange between these waves and the intensity of the object wave at the crystal output, as well

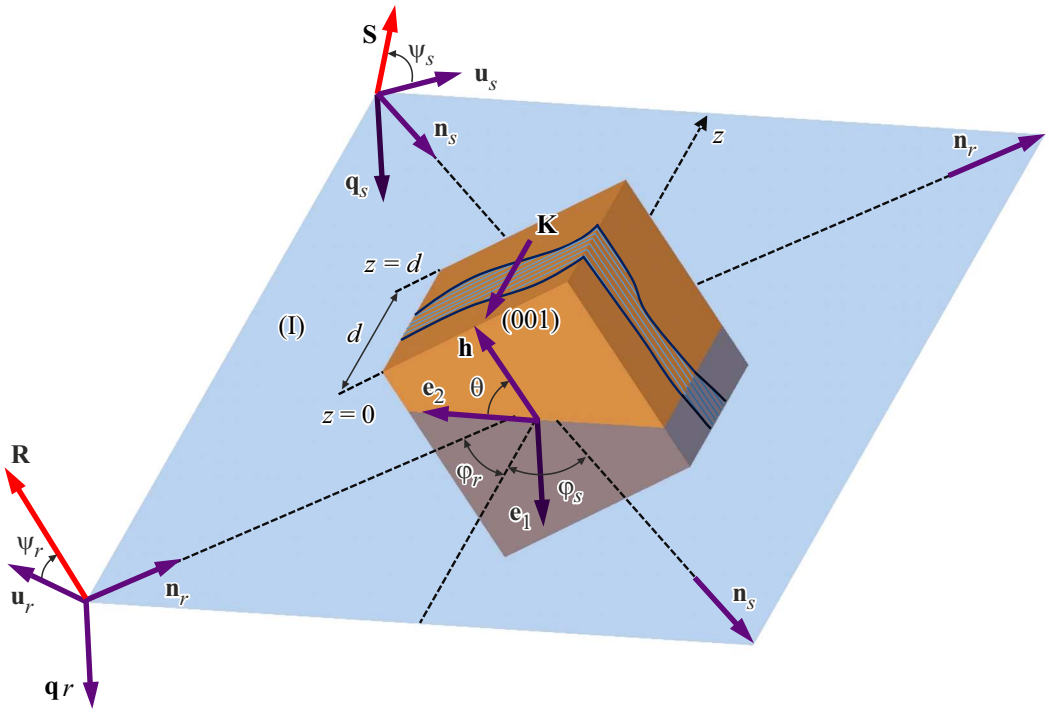

Figure 1. Schematic diagram of contra-directional two-wave mixing in the photorefractive (001) cut BSO crystal.

as to define the technique for numerical solving the coupled-wave equations that gives the most accurate coincidence of theoretical results with the experiment.

Thus, the goal of this work is to study the laws of energy exchange in the case of contra-directional two-wave mixing in a cubic photorefractive crystal of the 23 symmetry class at different orientation angles of the crystal and azimuths of the linear polarization of light waves. The theoretical results presented in the study are obtained on the basis of numerical solution to the coupled-wave equations performed in the approximation of static grating (without consideration to the self-diffraction) and in the dynamic approximation (with consideration to the self-diffraction). To validate the results of numerical calculations, the intensity of the object wave as a function of its polarization azimuth was investigated experimentally for different orientation angles of the crystal.

2. Theoretical model

Let us assume two monochromatic linearly polarized reference (subscript r) and object (subscript s) light waves (see Fig. 1) are incident on opposite antireflection coated faces of a crystal. Triads of unit vectors $(\mathbf{q}_r, \mathbf{u}_r, \mathbf{n}_r)$ and $(\mathbf{q}_s, \mathbf{u}_s, \mathbf{n}_s)$ are orthogonal bases, which are used to determine vector amplitudes of light waves. Directions of unit vectors $\mathbf{n}_r$ and $\mathbf{n}_s$ coincide with wave normals of the reference and object waves, respectively. Vector amplitude $\mathbf{R}$ of the reference wave lays in the plane formed by vectors $\mathbf{q}_r$ and $\mathbf{u}_r$, and forms azimuth ψ_r with vector $\mathbf{u}_r$, which is counted counterclockwise when facing vector $\mathbf{n}_r$. Azimuth ψ_s is the angular distance between unit vector $\mathbf{u}_s$ and vector amplitude $\mathbf{S}$ of the object wave, which is counted counterclockwise when facing vector $\mathbf{n}_s$.

The plane of incidence (I) in Fig. 1 is parallel to the surface of holographic table and perpendicular to working faces of the crystal. Unit vectors $\mathbf{e}_1$ and $\mathbf{e}_2$ belong to the orthogonal basis $(\mathbf{e}_1, \mathbf{e}_2, \mathbf{e}_3)$, which is rigidly fixed in relation to the surface of the holographic table. The direction of unit vector $\mathbf{e}_3$ (not shown in Fig. 1) coincides with axis Oz, along which the crystal thickness d is counted. Unit vector $\mathbf{h}$ is rigidly fixed in the crystallographic coordinate system and used to define position of the crystal in relation to the surface of the holographic table by means of the orientation angle θ, which is counted from vector $\mathbf{e}_2$ to vector $\mathbf{h}$, as shown in Fig. 1. Parallel lines on the crystal faces perpendicular to the (001) cut plane schematically represent the periodically arranged phase planes of the hologram that scatter light wave fronts. Wave vector $\mathbf{K}$ of the reflection hologram has a direction opposite to that of vector $\mathbf{e}_3$ and perpendicular to the (001) cut plane.

We represent vector amplitudes $\mathbf{R}$ and $\mathbf{S}$ of linearly polarized reference and object light waves mixing in the crystal as follows:

$$\mathbf{R} = (R_1\mathbf{q}_r + R_2\mathbf{u}_r)\exp(i\vartheta_r), \tag{1}$$

$$\mathbf{S} = (S_1\mathbf{q}_s + S_2\mathbf{u}_s)\exp(i\vartheta_s), \tag{2}$$

where $R_{1,2}$ and $S_{1,2}$ are scalar components of vector amplitudes $\mathbf{R}$ and $\mathbf{S}$, respectively; $\vartheta_{r,s}$ are initial phases of the reference and object waves.

The arising of volume holographic gratings is caused by the formation of a space charge in the nonuniform light field due to the presence of impurity centers in the band gap of the photorefractive crystal [24]. In the case of photoexcitation the electric charge carriers leave the illuminated bands as a result of diffusion and are captured by the traps in unilluminated bands. In the simplest case the donors and traps can be impurities of ions of the same type of atoms, but in different valence state [2]. With the use of single-level band model of photorefractive crystal, the first harmonic amplitude of electric field E_{sc} of the space charge of the photorefractive crystal can be obtained by the following formula:

$$E_{sc} = -im\frac{E_D}{1+E_D/E_q}. \quad (3)$$

where $E_D = k_bTK/e$, $E_q = eN_A/(\varepsilon K)$, $K = 2\pi/\Lambda$. Here, we have adopted the following notations: E_D — strength of the diffusive electric field; E_q — strength of the saturation electric field of traps; m — modulation depth of the fringe pattern; i — imaginary unit; K — modulus of the hologram wave vector; k_b — Boltzmann constant; T — absolute temperature; e — elementary electric charge; N_A — acceptor density; ε — dielectric permittivity of the crystal; Λ — spatial period of the holographic grating.

In the approximation of slowly changing amplitudes, coupled-wave equations can be obtained from the wave equation for optically active media using expressions (1)–(3):

$$\frac{dR_1}{dz} = ie^{-i\delta}\kappa_{r1s1}S_1 + ie^{-i\delta}\kappa_{r1s2}S_2 + \rho_r R_2 - \alpha_r R_1, \quad (4)$$

$$\frac{dR_2}{dz} = ie^{-i\delta}\kappa_{r2s1}S_1 + ie^{-i\delta}\kappa_{r2s2}S_2 - \rho_r R_1 - \alpha_r R_2, \quad (5)$$

$$\frac{dS_1}{dz} = ie^{i\delta}\kappa_{s1r1}R_1 + ie^{i\delta}\kappa_{s1r2}R_2 + \rho_s S_2 - \alpha_s S_1, \quad (6)$$

$$\frac{dS_2}{dz} = ie^{i\delta}\kappa_{s2r1}R_1 + ie^{i\delta}\kappa_{s2r2}R_2 - \rho_s S_1 - \alpha_s S_2, \quad (7)$$

where

$$\kappa_{mknt} = -\kappa_0(\mathbf{e}^*_{mk}\Delta\varepsilon^{-1}\mathbf{e}_{nt})/\cos\varphi_m,$$

$$\rho_{r,s} = (\rho+i\chi)/\cos\varphi_{r,s}, \quad \alpha_{r,s} = \alpha/\cos\varphi_{r,s}.$$

κ_{mknt} parameters are the coefficients of coupling between the linearly polarized light waves mixing on the reflection grating, where $m, n = r, s$; $k, t = 1, 2$. κ_0 parameter is the coupling constant and can be obtained from the following expression: $\kappa_0 = \pi n_0^3/(2\lambda)$, where λ is wavelength, c is speed of light in vacuum. Mutual coupling between components of vector amplitudes of the reference and object waves is determined through tensor convolutions $(\mathbf{e}^*_{mk}\Delta\hat{\varepsilon}^{-1}\mathbf{e}_{nt})$, where $\Delta\hat{\varepsilon}^{-1}$ is the change in inverse tensor of dielectric permittivity, which components can be obtained on the basis of the expressions presented in [5]. Angular distances φ_r, φ_s correspond to Bragg angles and lay in the plane I between the axis Oz and directions of vectors $\mathbf{n}_r$, $\mathbf{n}_s$.

In coupled-wave equations (4)–(7), constants ρ, α and χ denote specific rotation of polarization plane of light waves, natural absorption and circular dichroism of the crystal, respectively.

We used the following physical parameters of the BSO crystal in the theoretical calculations: refractive index of an unperturbed crystal $n_0 = 2.54$ at $\lambda = 633\cdot10^{-9}$ m [2]; electrooptic coefficient $r_{41} = 5\cdot10^{-12}$ m/V [2]; elasticity coefficients $c_1 = 12.96\cdot10^{10}$ N/m^2, $c_2 = 2.99\cdot10^{10}$ N/m^2, $c_3 = 2.45\cdot10^{10}$ N/m^2 [25]; photoelasticity coefficients $p_1 = -0.16$, $p_2 = -0.13$, $p_3 = -0.12$, $p_4 = -0.015$ [26]; piezoelectric coefficient $e_{14} = 1.12$ C/m^2 [25]. Here, we have adopted the following notations for nonzero components of tensors of the linear electrooptic ($\hat{r}^S$), photoelastic ($\hat{p}^E$) and inverse piezoelectric ($\hat{e}$) effects, as well as components of the elasticity tensor ($\hat{c}^E$):

$$r^s_{123} = r^s_{132} = r^s_{213} = r^s_{231} = r^s_{312} = r^s_{321} \equiv r_{41},$$

$$p^E_{11} = p^E_{22} = p^E_{33} \equiv p_1, \quad p^E_{12} = p^R_{23} = p^E_{31} \equiv p_2,$$

$$p^E_{13} = p^E_{21} = p^E_{32} \equiv p_3, \quad p^E_{44} = p^E_{55} = p^E_{66} \equiv p_4,$$

$$e_{123} = e_{132} = e_{213} = e_{231} = e_{312} = e_{321} = e_{312} = e_{321} \equiv e_{14}, \quad c^E_{11} = c^E_{22} = c^E_{33} = c_1,$$

$$c^E_{12} = c^E_{13} = c^E_{23} = c^E_{21} = c^E_{31} = c^E_{32} \equiv c_2,$$

$$c^E_{44} = c^E_{55} = c^E_{66} \equiv c_3.$$

The superscript S for the tensor of linear electrooptic effect $\hat{r}^S$ means that the r_{41} component was measured for the clamped crystal; components of the elasticity $\hat{c}^E$ and photoelastic effect $\hat{p}^E$ tensors were measured at a constant electric field. The orientation angle θ was obtained in assumption that unit vector $\mathbf{h}$ is parallel to one of crystallographic axes perpendicular to the [001] direction.

As a result of numerical solving the coupled-wave equations (4)–(7), S_1 and S_2 components of vector amplitude $\mathbf{S}$ of the object waves were obtained at the output of the crystal ($z = 0$). Initial conditions for solving the two-point boundary problem were chosen as follows: $R_1(0) = -R\cos\psi_r$, $R_2(0) = R\sin\psi_r$, $S_1(d) = -S\cos\psi_s$, $S_2(d) = S\sin\psi_s$. Coupled-wave equations (4)–(7) were numerically solved using the well-known shooting method [27].

3. Description of the experimental scheme

To study features of the mutual transformation of linearly polarized light waves in the case of their contra-directional mixing in a cubic photorefractive crystal, an experimental setup shown in Fig. 2 was used. In our investigations we used a specimen of BSO crystal of the (001) cut with a thickness of 3.73 mm. The choice of crystal cut is caused by the fact that with small thickness values the highest intensities of the object wave at the output of the

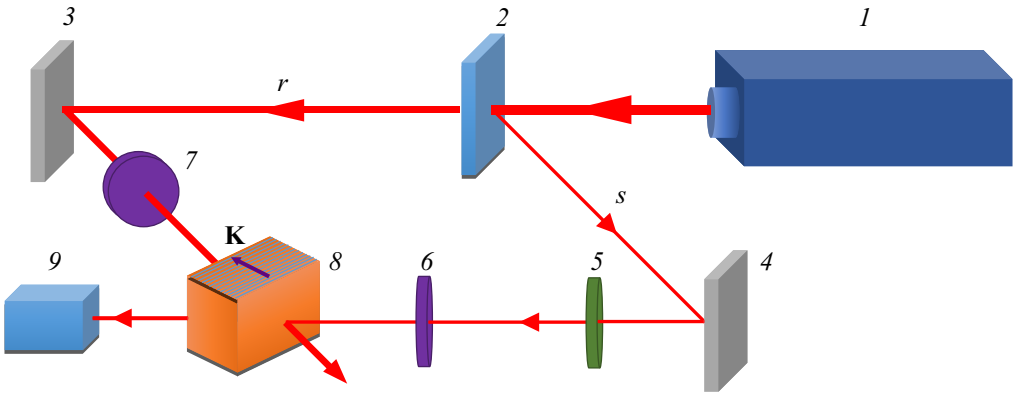

Figure 2. Schematic diagram of the experimental setup: *1* — helium-neon laser, *2* — light beamsplitter; *3, 4* — mirrors; *5* — phase half-wave plate; *6, 7* — orifice plates; *8* — BSO crystal; *9* — FD-7K photodiode.

crystal with appropriate choice of input linear polarization azimuths of light waves in the BSO crystal are achieved in the case when wave vector **K** of the reflection hologram is directed along one of crystallographic directions of the ⟨100⟩ family (see [28]). Thickness of the crystal specimen was chosen in such a way as to have the rotation angle of polarization plane of light waves during their propagation in the crystal approximately equal to $\rho d \approx \pi/2$. The choice of this thickness is caused by the fact that with the above-specified condition fulfilled, the intensity of the object wave at the output of the crystal is at its maximum level [28].

Procedure of the experiment was as follows. The light beam from the helium-neon laser *1* radiating at a wavelength of 632.8 nm was splitted by beamsplitter *2* into reference *r* and object s beams. These beams, having reflected from mirrors *3* and *4*, passed through the orifice plates *6, 7* installed on their path and mixed in BSO crystal *8* forming a reflection hologram with wave vector **K** in the crystal. In the experiment the reference light beam was polarized in the plane of incidence. The polarization of the object light beam before it enters the crystal was controlled by phase half-wave plate *5*. Behind the crystal, on the path of the object beam propagation, as a recorder of the light intensity, photodiode *9* of FD-7K type was installed being connected into a measuring circuit with a digital voltmeter.

In the course of experimental investigations a procedure similar to that of [29] was used. Prior to the start of the holographic experiment, the intensity of the object beam at the output of the crystal was measured by the digital voltmeter without the reference beam and the reading of I_s^0 was recorded. Then the crystal was continuously illuminated by the reference and object beams for a period of tine $\tau \approx 30$ s, during which the light-sensitive area of photodiode *9* was obscured by an opaque screen. Within this period, a photoexcitation took place in the crystal and electric charge carriers were redistributed over the defect centers, which resulted in formation of a spatially nonuniform distribution of the charge [24,2]. The electric field formed inside the photorefractive crystal through the combined action of linear electrooptic, photoelastic and inverse piezoelectric effects provided the recording of a reflection hologram. After a 30-second hold time, the opaque screen in front of the photodiode was removed and the light-sensitive area was exposed to the object beam. The intensity of the object beam was measured at this moment in presence of the reference beam with a fixed I_s. Then the polarization azimuth ψ_s was changed and the above sequence of actions of the experiment repeated. Numerical value of the relative intensity of the object wave was determined as $\gamma = I_s/I_s^0$.

If γ is equal to 1, it means that intensity of the object wave at the output of the crystal is equal to its intensity at the input of the crystal. If γ is greater than unit, then in the case of contra-directional two-wave mixing the energy is transferred from the reference wave to the object wave and the object wave is amplified. For example, with $\gamma = 1.05$ the intensity of the object wave at the output of the crystal will be 105% in relation to its initial level, i.e. the intensity of the object wave at the output of the crystal will be higher than its intensity at the input of the crystal. With $\gamma < 1$ the energy exchange between coupled-waves takes place in the reverse direction and the intensity of the object wave decreases in relation to its initial level.

Prior to the start of the holographic experiment, we have evaluated by test the parameters of specific rotation, natural absorption and circular dichroism of the BSO specimen used and the following results were obtained: $\rho = 384$ rad/m, $\alpha = 15\,\mathrm{m}^{-1}$, $\chi = 1.5\,\mathrm{m}^{-1}$. In the process of experiment, Bragg angles in the crystal were $\varphi_r = \varphi_s = 2.5°$, while the ratio of intensities of the object and reference waves was 1 : 6.

4. Results and discussion

Plots of dependencies *1* and *4* in Fig. 3 represent envelopes of maximum (curve *1*) and minimum (curve *4*) values of the relative intensity γ, that were obtained as a

result of scanning over the values of orientation angle θ at each polarization angle ψ_s set at $z = d$. Curves *2* and *3* correspond to plots of the dependence of the relative intensity γ on polarization azimuth ψ_s calculated at $\theta = -4°$ (curve *2*) and $\theta = 86°$ (curve *3*).

In the process of numerical solving the coupled-wave equations (4)–(7), values of orientation angle θ, polarization angle ψ_r and ψ_s were selected as follows. Contrast of the recording fringe pattern is optimum if with light waves propagating in the crystal vector amplitudes **R** and **S** remain parallel to each other ($\mathbf{R} \parallel \mathbf{S}$) at any z [21]. Therefore, the origin of azimuth ψ_s in the calculations and in the experiment was selected equal to a value of this azimuth where the condition of $\mathbf{R} \parallel \mathbf{S}$ was fulfilled. To find this origin, the rotation angle of the polarization plane of light waves was measured during their propagation in the BSO test specimen, which turned to be equal approximately to 82°.

Since it was assumed that the reference wave at $z = 0$ was polarized in the plane of incidence ($\psi_r = 0°$), its azimuth at $z = d$ was respectively equal to 82°. The condition of $\mathbf{R} \parallel \mathbf{S}$ is fulfilled if at $z = d$ azimuth ψ_s is equal to 98°, which was taken as the origin. A decrease in ψ_s results in an angle of $(98° - \psi_s)$ formed between vector amplitudes **R** and **S** inside the crystal. For example, at $\psi_s = 8°$ vector amplitudes **R** and **S** inside the crystal are perpendicular to each other ($\mathbf{R} \perp \mathbf{S}$). At $\psi_s = -82°$ vector amplitudes **R** and **S** are parallel to each other.

Plots shown in Fig. 3, *a* are calculated without consideration to the self-diffraction of recording light waves on the hologram formed in the photorefractive crystal (the approximation of static grating). For the numerical solving the coupled-wave equations (4)–(7), it was assumed that the recording fringe pattern inside the crystal over the z coordinate is predetermined and has the simplest periodic structure of the following form: $I(z) = I_0[1 + m\cos(Kz)]$, where I_0 is mean light intensity, which is constant along the axis Oz, K is modulus of the hologram wave vector. The modulation depth m is determined only by intensities of light waves at the input of the crystal and is constant at any z coordinate inside the crystal ($m(z) = \text{const}$).

As can be seen from Fig. 3, *a*, the highest (curve *1*) and the lowest (curve *4*) values of the relative intensity γ are independent of the azimuth ψ_s. It means that in the approximation of static grating γ achieves equally highest values at both $\mathbf{R} \parallel \mathbf{S}$ and $\mathbf{R} \perp \mathbf{S}$. Extreme points of the $\gamma(\psi)$ dependence plots obtained at $\theta = -4°$ (curve *2*) and $\theta = 86°$ (curve *3*) coincide with each other in terms of value of γ, however the curves are shifted in relation to each other by an angle of π. The solution to coupled-wave equations (4)–(7) in the approximation of static grating predicts that at any polarization azimuth ψ_s, by changing the orientation angle θ, the object wave can be either amplified or attenuated.

Coupled-wave equations (4)–(7) written with consideration to the effect of self-diffraction of recording light waves on the holographic grating formed in the photorefractive

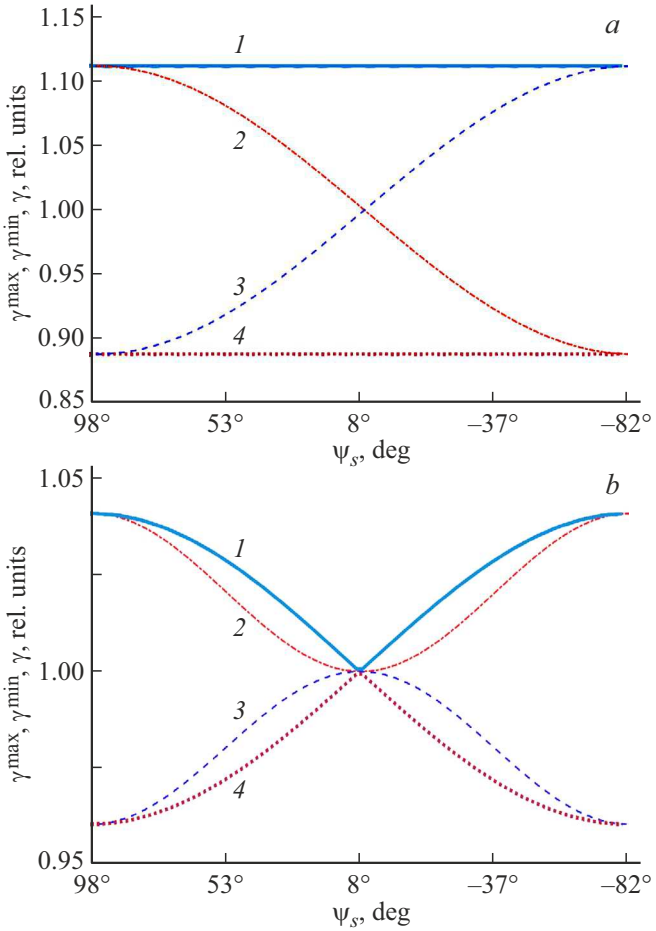

Figure 3. Plots of dependencies of the relative intensity of the object wave calculated at $\theta = -4°$ (curve *2*) and $\theta = 86°$ (curve *3*), as well as dependencies of its maximum (curve *1*) and minimum (curve *4*) values on polarization angle ψ_s of the object wave: *a* — approximation of static grating, *b* — dynamic approximation.

crystal (hereinafter referred to as the „dynamic approximation“) were used to calculate the plots of dependencies shown in Fig. 3, *b*. Generally, the typical time of holographic grating recording in a photorefractive crystal is much greater than the time of light wave passage through the specimen thickness [2]. Therefore, the arising diffraction processes can be considered as quasi-stationary ones and coupled-wave equations (4)–(7) can be used to calculate components of vector amplitudes of the reference and object waves, which are slowly changing functions of z coordinate.

Let us consider that the recording fringe pattern and holographic grating achieve some interconsistent state. Then, according to expression (3), in the linear mode of recording the amplitude of holographic grating is proportional to the depth of modulation m of the recording fringe pattern, which is a function of z coordinate in the dynamic approximation ($m(z) \neq \text{const}$).

As it follows from Fig. 3, *b*, in the dynamic approximation, the highest and the lowest values of γ optimized with

respect to orientation angle θ become functions of ψ_s. The highest value of γ is achieved in the case when $\mathbf{R} \parallel \mathbf{S}$. If $\mathbf{R} \perp \mathbf{S}$. there is no energy exchange during contra-directional two-wave mixing ($\gamma = 1$). The plot of $\gamma(\psi_s)$ obtained in the dynamic approximation at $\theta = -4°$ (curve *2* in Fig. 3, *b*) is significantly different from the similar dependence obtained in the approximation of static grating (curve *2* in Fig. 3, *a*) — at any azimuth ψ_s the condition of $\gamma \geq 1$ is fulfilled. With $\theta = 86°$ (curve *3* in Fig. 3, *b*) γ is not greater than unit, which means that the object wave is attenuated at any azimuth ψ_s. In the similar plot obtained in the approximation of static grating (curve *3* in Fig. 3, *a*), γ can be greater than unit, depending on the orientation angle θ.

It should be noted that azimuths $\psi_s = 98°$ and $-82°$ in fact correspond to the same direction of vector amplitude of the object wave, because the vector amplitude is the amplitude multiplied by the polarization vector, which is bidirectional. Solving the problem in the approximation of static grating gives different directions of the energy exchange between waves for the same polarization vector (see Fig. 3, *a*): with $\psi_s = 98°$ the object wave is amplified ($\gamma > 1$), while with $\psi_s = -82°$ the object wave is attenuated ($\gamma < 1$). It is clear that opposite directions of the energy exchange can not correspond to the same direction of the polarization vector of the object wave, and it emphasizes shortages of the use of the approximation of static grating to solve coupled-wave equations. In the case of dynamic approximation azimuths of $\psi_s = 98°$ and $-82°$ have the same correspondent value of γ (see Fig. 3, *b*), which points to the fact that the numerical solution to coupled-wave equations in the dynamic approximation makes it possible to obtain theoretical results that match qualitative ideas of physical mechanism of the energy exchange in the case of contra-directional two-wave mixing.

To test validity of the theoretical curves shown in Fig. 3, we have investigated experimentally the $\gamma(\psi_s)$ dependencies for orientation angles $\theta = -4°$ (Fig. 4, *a*) and $\theta = 86°$ (Fig. 4, *b*). Triangles and dots represent the results of two series of the $\gamma(\psi_s)$ dependence experimental plotting. As can be seen from the experiment, with $\theta = -4°$ the highest γ is equal to 1.04, while its minimum value is approximately equal to unit (≈ 0.996). With $\theta = 86°$ the highest relative intensity γ is approximately equal to unit (≈ 1.004), while its minimum value is -0.947. It is impossible to achieve coincidence between the plots of $\gamma(\psi_s)$ dependencies obtained in the approximation of static grating and the experimental data, because the periodicity of the theoretically obtained plots (see curves *2* and *3* in Fig. 3, *a*) does not coincide with the experimental curves (Fig. 4). In addition, the relative intensity γ in the approximation of static grating at any azimuth ψ_s, due to the appropriate choice of the orientation angle θ, can vary from maximum possible value to minimum possible value, which does not correspond to the experimental data shown in Fig. 4.

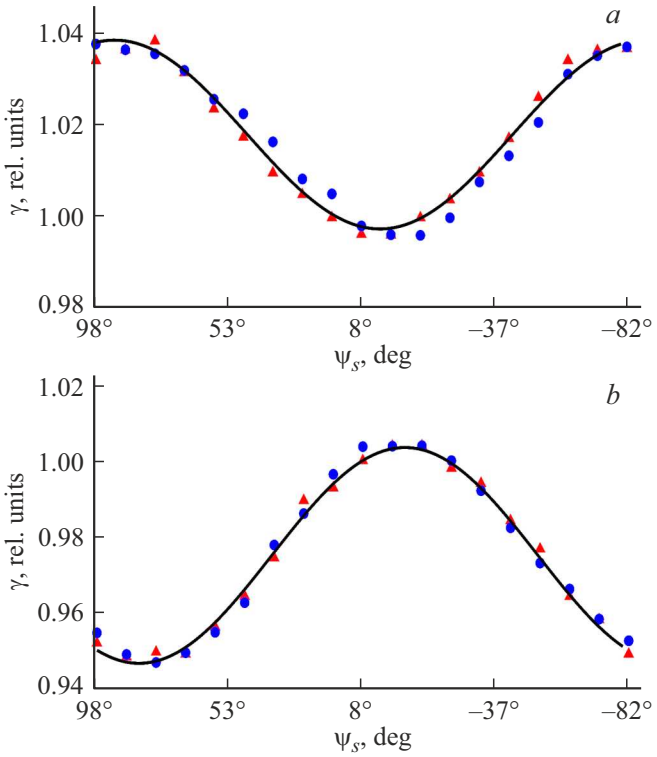

Figure 4. Plots of relative intensity γ of the object waves as a function of polarization azimuth ψ_s calculated at $\theta = -4°$ (*a*) and $\theta = 86°$ (*b*): solid line — theoretical curve; triangles and dots correspond to experimental data.

Solid lines in Fig. 4 represent plots of the $\gamma(\psi_s)$ dependence obtained from solving the coupled-wave equations (4)–(7) in the dynamic approximation. As it follows from the plotting, the obtained dependence plots match the experimental data quite accurately. With the $\mathbf{R} \parallel \mathbf{S}$ condition fulfilled, the highest relative intensities γ are achieved at $\theta = -4°$, while the lowest values are achieved at $\theta = 86°$. With $\mathbf{R} \perp \mathbf{S}$, as predicted theoretically in the dynamic approximation, the experimentally determined relative intensity γ is approximately equal to unit. Also, the periodicity of theoretical and experimental plots of the $\gamma(\psi_s)$ is matched well. Thus, the consideration of self-diffraction of light waves makes it possible to achieve an accurate coincidence between results of numerical calculations and experimental data.

The values of relative intensity γ obtained in this study are quite low. At the same time, it is worth to note that γ can be increased significantly by changing the structure of impurity centers in the band gap when doping the photorefractive crystal, as well as by changing the spatial period of the reflection holographic grating [2,30].

5. Conclusion

The coupled-wave equations (4)–(7), which can be used to find vector amplitudes of the reference and object

light waves in case of their contra-directional mixing in a photorefractive crystal of the 23 symmetry class, are derived with consideration to the combined contribution from the linear electrooptic, photoelastic, inverse piezoelectric effects, optical activity, natural absorption of the crystal, as well as circular dichroism. These equations are solved numerically in the approximation of predetermined grating (without consideration to the self-diffraction) and in the dynamic approximation (with consideration to the self-diffraction).

The dependence of relative intensity of the object wave on azimuth of its linear polarization is investigated theoretically and experimentally at a fixed linear polarization of the reference wave in the plane of incidence. It is shown that in general only the use of dynamic approximation for solving the coupled-wave equations (4)–(7) allows achievement of the best matching between theoretical and experimental data. Results obtained in the approximation of static grating and in the dynamic approximation can only coincide when vector amplitudes of the reference and object waves remain parallel to each other ($\mathbf{R} \parallel \mathbf{S}$) during propagation of the waves in the crystal. In other cases ignoring the effect of recording light waves self-diffraction on the recorded holographic grating results in error in the calculations of the object wave intensity at the output of the crystal.

The case of contra-directional two-wave mixing in the BSO crystal of (001) cut studied in [21–23] with the $\mathbf{R} \parallel \mathbf{S}$ condition fulfilled inside the crystal is the optimum case, because it is the fulfillment of this condition that makes possible the achievement of the highest relative intensities of the object wave. The analysis of contra-directional two-wave mixing with fulfillment of the $\mathbf{R} \perp \mathbf{S}$ condition is of no interest, because the energy exchange between coupled-waves is nearly absent, as confirmed by experiments.

The obtained results can be useful for modelling the mutual transformation of light waves in case of their contra-directional two- and four-wave mixing in a cubic photorefractive crystal. In addition, the presented data allows more accurate prediction of the relative intensity of the object light wave at the output of the crystal and determining the conditions of holographic experiment that give the highest level of this intensity.

Acknowledgments

The author thanks reviewers for thorough reading of the manuscript and proposed comments that allowed noticeable improvement of the research level of this study.

Funding

The study was financially supported by the Ministry of Education of the Republic of Belarus (agreement dated March 22, 2021 No. 1410/2021) within the State Program of Scientific Research No. 6 „Photonics and electronics for innovations“ for 2021–2025. (assignment 6.1.14).

Conflict of interest

The authors declare that they have no conflict of interest.

References

[1] S.M. Shandarov, N.I. Burimov, Yu.N. Kulchin, R.V. Romashko, A.L. Tolstik, V.V. Shepelevich. Kvantovaya elektron. **38**, *11*, 1059 (2008). (in Russian).
[2] M.P. Petrov, S.I Stepanov, A.V. Khomenko. Fotorefraktivnyie krictally v kogerentnoy optike. Nauka, SPb. (1992). 320 p. (in Russian).
[3] V.M. Petrov, A.V. Shamray. Interferentsiya i diffraktsiya dlya interferentsionnoy fotoniki. Lan, SPb (2019). 460 p. (in Russian).
[4] A.A. Izvanov, A.E. Mandel, N.D. Khatkov, S.M. Shandarov. Avtometriya. **2**, 79 (1986). (in Russian).
[5] S.M. Shandarov, V.V. Shepelevich, N.D. Khatkov. Optika i spektroskopiya **70**, *5*, 1068 (1991). (in Russian).
[6] S.I. Stepanov, S.M. Shandarov, N.D. Khatkov. FTT **29**, *10*, 3054 (1987). (in Russian).
[7] V.V. Shepelevich, S.M. Shandarov, A.E. Mandel. Ferroelectrics **110**, 235 (1990).
[8] V.V. Shepelevich. Zhurn. prikl. spektr. **78**, *4*, 493 (2011). (in Russian).
[9] V.I. Burkov, Yu.F. Kargin, V.A. Kizel, V.I. Sitnikova, V.M. Skorikov. Pis'ma v ZhETF **38**, *7*, 326 (1988). (in Russian).
[10] B.V. Bokut, G.S. Mityurich, V.V. Shepelevich. Dokl. AN BSSR **23**, *6*, 507 (1979). (in Russian).
[11] P.P. Khomutovski, V.V. Shepelevich. Proc. SPIE **3347**, 84 (1998).
[12] A.A. Firsov, V.V. Shepelevich. Vesn. Mozyrskogo gos. ped. un-ta **1**, 21 (2005). (in Russian).
[13] V.N. Naunyka, V.V. Shepelevich, S.M. Shandarov. Optika i spektroskopiya **129**, *1*, 66 (2021). (in Russian).
[14] R.V. Litvinov. Kvantovaya elektron. **37**, *2*, 154 (2007). (in Russian).
[15] H. Lordue G., J.A. Gomez, A. Salazar. Opt. Commun. **284**, 446 (2011).
[16] N.M. Kozhevnikov. Optika i spektroskopiya **117**, *6*, 983 (2014). (in Russian).
[17] S. Plaipichita, P. Buranasiria, C. Ruttanapuna, P. Jindajitawata. Integrated Ferroelectrics **156**, *1*, 150 (2014).
[18] M.A. Bryushinin, V.V. Kulikov, I.A. Sokolov, P. Delaye, G. Pauliat. FTT **56**, *6*, 1158 (2014). (in Russian).
[19] N. Katyal, Natasha, A. Kapoor. Optik **126**, 5941 (2015).
[20] V.V. Davydovskaya, V.V. Shepelevich. Vestn. Polotskogo gos. un-ta. Ser. C **12**, 54 (2018). (in Russian).
[21] S. Mallick, M. Miteva, L. Nikolova. J. Opt. Soc. Am. B **14**, *5*, 1179 (1997).
[22] M. Weber, E. Shamonina, K.H. Ringhofer, G. von Bally. Opt. Mater **18**, 119 (2001).
[23] V.V. Shepelevich, V.N. Naunyka, S.F. Nichiporko, S.M. Shandarov, A.E. Mandel. Pis'ma v ZhTF **29**, *18*, 22 (2003). (in Russian).
[24] N.V. Kukhtarev, V.B. Markov, S.G. Odulov, M.S. Soskin, V.L. Vinetskii. Ferroelectrics **22**, 949 (1979).

[25] K.S. Aleksandrov, V.S. Bondarenko, M.P. Zaitseva, B.P. Sorokin, Yu.I. Kokorin, V.M. Zrazhevsky, A.M. Sysoev, B.V. Sobolev. FTT **26**, *12*, 3603 (1984). (in Russian).
[26] G.A. Babonas, A.A. Reza, E.I. Leonov, V.I. Shandaris. ZhTF **55**, *6*, 1203 (1985). (in Russian).
[27] Y.H. Ja. Opt. Quant. Electron. **15**, 529 (1983).
[28] V.N. Naunyka, V.V. Shepelevich. Pis'ma v ZhTF **33**, *17*, 16 (2007). (in Russian).
[29] V.V. Shepelevich, N.N. Egorov. Pis'ma v ZhTF **17**, *5*, 24 (1991). (in Russian).
[30] L. Solymar, D.J. Webb, A. Grunnet-Jepsen. The physics and applications of photorefractive materials. Clarendon Press, Oxford. (1996). 493 p.

Translated by Y.Alekseev